

20. DIAGENESIS AND DEWATERING OF CLAY-RICH SEDIMENTS, BARBADOS ACCRETIONARY PRISM¹

Roy Wilkens,² Patrick McLellan,³ Kate Moran,⁴ Jane Schoonmaker Tribble,⁵ Elliott Taylor,^{6,7}
and Elizabeth Verduzco⁸

ABSTRACT

Physical properties measurements of samples from the toe of the Barbados accretionary prism were combined with data from an earlier Barbados drilling study. Examination of porosity and velocity profiles in the light of both empirical and theoretical relationships leads to several conclusions:

1. The initial stages of deformation at the tip of the accretionary prism do not result in a substantial loss of porosity for the accreted sediments. Within 5 km of the toe of the accretionary prism, porosity profiles are similar to profiles at reference sites seaward of the deformation when variations in lithology are considered. Further from the prism toe, within the accretionary wedge (15–20 km), porosity profiles exhibit a loss of approximately 5% porosity relative to the reference sites.

2. The décollement and most of the other major thrusts penetrated in the prism are associated with Miocene sedimentary sections because of the higher porosity of those sediments and not because of some diagenetic change associated with cementation. The relatively high porosities correlate with abundant smectite derived from volcanic ash alteration.

3. The Miocene lithology appears to compact more slowly than the sediments above and below them. This suggests that the porosity, and probably strength, difference between adjacent units may become greater with depth, resulting in an ever increasing tendency for the Miocene sediments to be the locus of slip in bedding-parallel faulting events as compaction proceeds.

INTRODUCTION

The accretion of sediments onto plate margins above subducting lithosphere is an important process in the evolution of the Earth's crust. High porosity, relatively uncemented sediments undergo dewatering and diagenesis within the accretionary prism, eventually becoming sedimentary and metamorphic rocks. Examples of the end products of this process are exposed and have been studied in many places in the world (Moore and Karig, 1980; Moore and Allwardt, 1980; Lundberg, 1982; Schoonmaker et al., 1986). Deep Sea Drilling Project (DSDP) operations at or near the deformation fronts of accretionary prisms along the Pacific rim (Lee et al., 1973; Bouma and Moore, 1975; Carson and Bruns, 1980; Shephard et al., 1981; Bray and Karig, 1986) and off Barbados (Marlow et al., 1984; Pudsey, 1984) have recovered samples of sediment that represent the beginning of the accretion process.

Leg 110 of the Ocean Drilling Program (ODP) saw a return to the Barbados accretionary wedge in an effort to augment data collected during DSDP Leg 78 (Marlow et al., 1984; Pudsey, 1984) and extend our understanding of the early stages of sedimentary accretion. Six sites were drilled during Leg 110 to add to the three sites of Leg 78 (Fig. 1). Of the total of nine sites

for the two legs, seven are within the accretionary prism and two reference sites are located to the east of the deformation front.

The results of Leg 110 drilling shed new light on problems left unresolved by Leg 78 and other accretion-directed drilling experiments. First, how much dewatering takes place in the initial stages of sediment offscraping and deformation? Westbrook et al. (1984) reasoned that because the rate of shortening and accretion appear to be greatest at the tip of the accretionary wedge, it is likely that much of the dewatering of the accreted sediments takes place in this area. Furthermore, they postulated high fluid pressures in the sediments below the décollement due to the dewatering of downgoing sediments. Investigators drilling in slope sediments above the accretionary wedge off of Japan (Arthur et al., 1980; Carson et al., 1982) observed sedimentary structures such as scaly cleavage and carbonate veining that pointed toward elevated fluid pressures within the accretionary prism. Results of the earlier Barbados accretionary wedge drilling (DSDP Leg 78) suggested that the sediments within the prism were not greatly dewatered even though the section had undergone deformation (Marlow et al., 1984). Physical properties and consolidation tests of samples from near the Nankai Trough prism toe (DSDP Leg 87) also revealed only a minor amount of sediment dewatering (Bray and Karig, 1986). Leg 110 results generally support the observation of minimal dewatering while looking at a much more extensive transect of the toe of the prism, penetrating the décollement and drilling farther away from the prism tip in the direction of the arc.

Penetration of the décollement eluded Leg 78 investigators due to drilling problems. There are several speculations as to why the décollement develops in a particular sedimentary horizon. It might be a zone of overpressured pore fluid resulting from a permeability contrast effectively limiting the dewatering of sediments deeper in the accretionary prism. An overpressure zone leads to an interval of low effective stress and shear strength in the sedimentary column (Hubbert and Rubey, 1959; Westbrook

¹ Moore, J. C., Mascle, A., 1990. *Proc. ODP, Sci. Results*, 110: College Station, TX (Ocean Drilling Program).

² Hawaii Institute of Geophysics, Honolulu, HI 96822.

³ Petro-Canada, P.O. Box 2844, Calgary, Alberta, T2P 3E3, Canada.

⁴ Bedford Institute of Oceanography, Dartmouth, Nova Scotia, B2Y 4A2 Canada.

⁵ Hawaii Institute of Geophysics, Honolulu, HI 96822.

⁶ Ocean Drilling Program, Texas A&M University, College Station, TX 77843.

⁷ Present address: School of Oceanography, University of Washington, Seattle, WA.

⁸ Wellesley College, Wellesley, MA 02257.

West

East

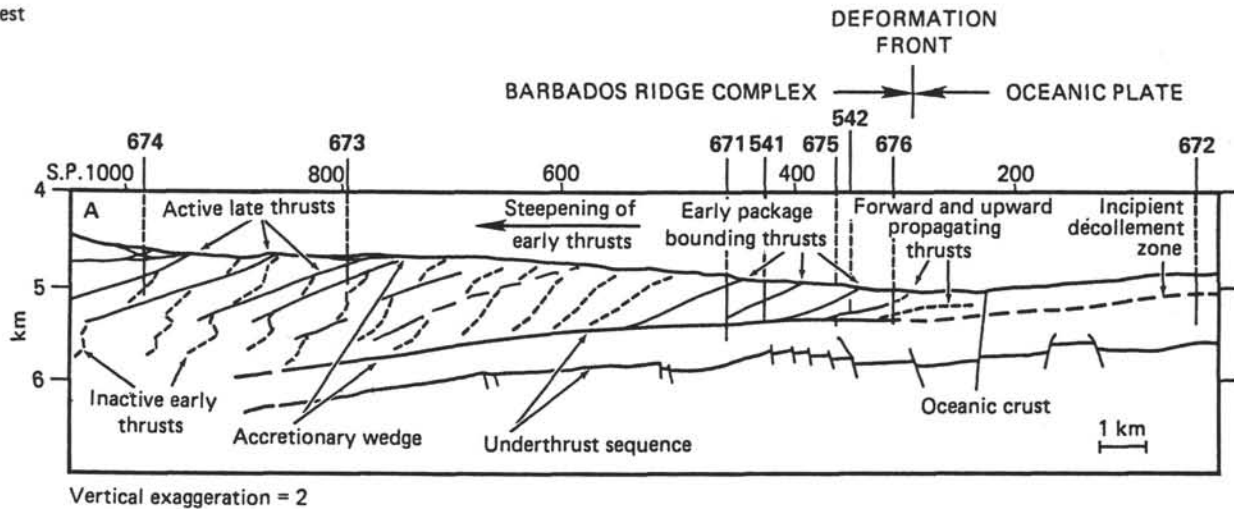


Figure 1. Cross-section of the Barbados accretionary wedge transect showing the locations of Leg 78 (Sites 541, 542) and Leg 110 (Site 671). Site 543 (not shown) is east of the deformation front but farther north than the sites included in this figure (from Moore, Mascle, et al., 1987).

and Smith, 1983; von Huene and Lee, 1983; Davis et al., 1983). Another possibility explaining the stratigraphic position of the décollement involves a diagenetic horizon. Softer, deformable sediments overlying more extensively cemented and lithified sedimentary rocks may present a contrast in sediment strength, with the upper sediments being accreted and the lower sediments subducted (Moore, Mascle, et al., 1975). Finally, the position of the décollement may reflect a local zone of weakness caused by differential compaction characteristics of differing sediment types, causing a local porosity maximum (Karig and Sharman, 1975; Pudsey, 1984).

Leg 110 penetrated or entered the detachment thrust at three sites as well as drilling through several major thrust faults within the accretionary prism (Fig. 1). In this study we examine the porosity and compressional-wave velocity profiles at each of the Leg 110 and Leg 78 sites using measurements of samples from recovered core. The relationship between velocity and porosity can be used to infer differences in strength among the sediment samples. Although the evidence is far from definitive, data suggest that the décollement and virtually all of the other major thrusts seen in the core are rooted in the same Miocene sedimentary units that are relatively richer in volcanically derived smectite (Pudsey, 1984; Tribble, this volume) and biogenic opal, resulting in relatively higher porosities and inferred lower strength than the surrounding sediments.

METHODS

The dewatering of the toe of the accretionary prism and mechanical aspects of the stratigraphic location of the décollement can be examined using the interrelationship between compressional-wave velocity and porosity measured at regular intervals in the core. Details of the measurement procedures are included in individual site chapters (Mascle, Moore et al., 1988). Briefly, the compressional-wave velocity was determined for samples removed from every other section of core. Measurements were made with the Hamilton Frame Velocimeter using the methods of Boyce (1976) modified by the addition of an electronic timing circuit of ODP design.

The index properties of bulk density, porosity, water content, and grain density were measured using an electronic balance (weight) and a gas-operated pycnometer (volume). The balance records multiple weights over a period of time, generally 10 to 20 s, and averages those values to eliminate accelerations due to the heave and roll of the ship. Repeated weighings of brass standards during the cruise showed the scale to be highly accurate and stable, with an error on the order of a few tenths of a percent.

The pycnometer, unfortunately, was neither accurate nor stable. Stability problems were minimized by repeating volume measurements of the same samples until three values agreed to within 1 percent. Accuracy also presented a problem. The grain density data listed in the site chapters are inconsistent with the listed porosities and bulk densities. Grain densities calculated from the listed porosities and bulk densities are commonly greater than 3.00 g/cm^3 . These values are unrealistically high given that none of the major mineralogical components of the sediments have a grain density greater than 2.80 g/cm^3 .

At Site 676 the individual index property samples were split. Half of each sample was measured using the pycnometer and the other half using Archimedes Principle (Boyce, 1976), the standard procedure used during the DSDP. A comparison of the two data sets is presented in Figure 2, showing that pycnometer-derived values of porosity, bulk density, and water content are larger than the results of older methods. While the differences between the two data sets were not more than a few percent, they were enough to complicate comparisons with data collected during Leg 78. The problem is illustrated in Figure 3, a plot of the density vs. the porosity of Pleistocene sediment samples from Site 671 (Leg 110) and Site 541 (Leg 78). Two sets of Site 671 data are presented; the original data and the data corrected using correlation equations from the Site 676 comparison data. The corrected data are in good agreement with the Leg 78 data and exhibit a range of grain densities that are reasonable for a clay-rich marine sediment. We have applied the correction formulas to all of the Leg 110 data and use the corrected values in further discussion and in figures. The reduction of the measured porosity and density values will not have any significant effect on the individual site chapter discussions of uncorrected physical properties as the correction preserves all of the relative differences between samples from Leg 110 sites.

POROSITY

Porosity vs. depth functions of oceanic sediments are greatly influenced by both physical and chemical composition (including mineralogy, grain size, and grain morphology) and the extent to which alteration has influenced those factors. The data from the two reference sites, Site 543 (Leg 78) and Site 672 (Leg 110), are displayed in Figure 4 with an empirical porosity-depth function for terrigenous silts and clays (Hamilton, 1976). The Hamilton porosity curve has been corrected using his estimation of sample rebound from *in situ* to laboratory to compare them to the Leg 110 and Leg 78 laboratory data. The terrigenous curve comes from a single DSDP site (Site 222) drilled 1300 m into the Indus Fan (Hamilton, 1976).

The empirical curve is assumed to represent a "normal" end-member compaction curve. Divergence from the curve (positive

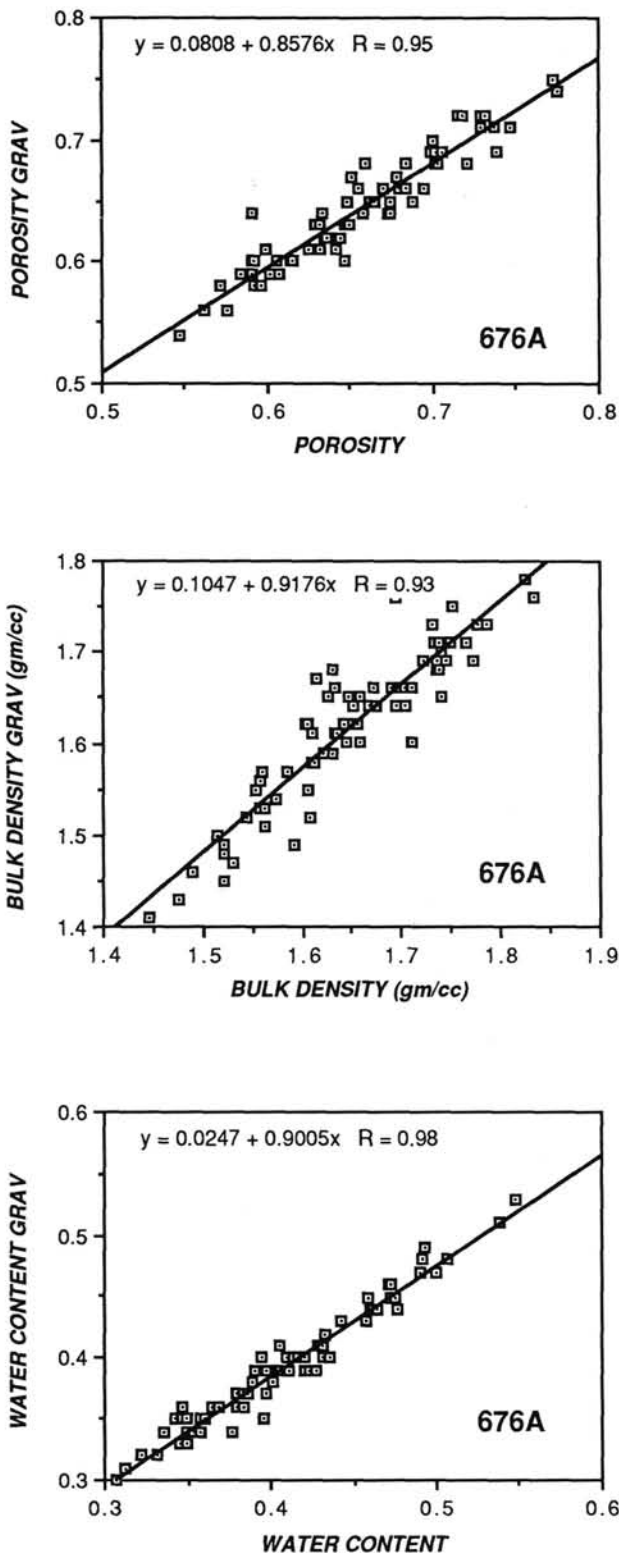


Figure 2. Comparison of index properties measured with two different volume determinations: pycnometer, and using Archimedes' Principle. The Y axes (grav) samples use the DSDP (Archimedes') method. Regressions of the data have a slope near 0.9 rather than 1.0.

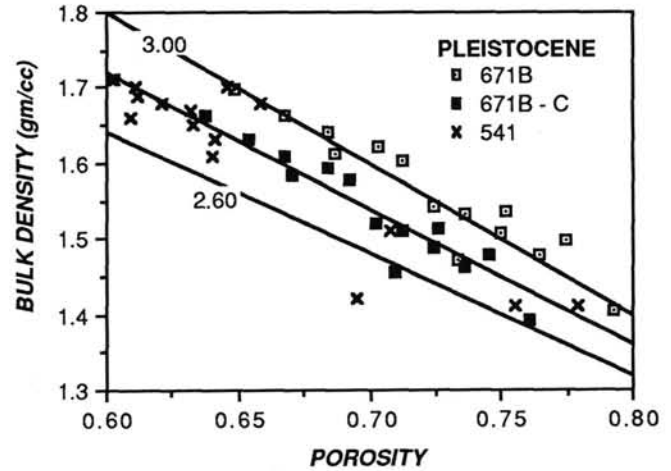


Figure 3. Bulk density vs. porosity for Pleistocene sediments from Site 671 (Leg 110) and Site 541 (Leg 78). The Site 671 values labeled C have been corrected according to relationships developed using Site 676 data (see Fig. 2). Lines of constant grain density have been superimposed on the plot. The original Site 671 data exhibit grain densities that are too large for samples that are predominantly clay.

or negative) may be caused by a change in the sediment composition, as in the Miocene sediments discussed below. Positive values may also be the result of either abnormal compaction, with sediments exhibiting excess porosity due to pore pressures greater than hydrostatic pressure, or of cementation of sediment grains, which signals a change in the regime of porosity reduction from purely mechanical consolidation to include dissolution and precipitation of mineral phases.

At both Sites 672 and 543 there is general agreement with the trend of the empirical curve for terrigenous clays, although the data, particularly at Site 672, are on the order of 5 to 10% less than the predicted porosity. Agreement between the Hamilton profile and Site 543 measurements may be misleading. Oligocene and older sediments at Site 543 contain greater amounts of biogenic silica (radiolarian tests) than any of the other Leg 78 or Leg 110 sites with the exception of Site 673. Radiolarian tests tend to hold open the sediment framework, resulting in higher porosities at depth than the terrigenous curve (Hamilton, 1976; Tada and Iijima, 1983). The difference in porosity at the top of Site 543 and at Site 672 may also be attributable to a somewhat different physical or chemical composition of the sediments in the Barbados region relative to Indus Fan sediment, or perhaps to the fact that the fan sediments undoubtedly accumulated at a much faster rate than at the oceanic reference sites and are less consolidated.

Sites 543 and 672 exhibit zones of anomalously high porosity associated with Miocene sediment. The Miocene sediments are compositionally distinct due to an abundance of smectite. Tribble (this volume) and Pudsey (1984) suggest that authigenic smectite (formed as a result of volcanic ash alteration) may cause sediments to exhibit relatively large porosities due to their ability to absorb quantities of interlayer water. Analytical data show a coincidence of smectite concentrations and relative porosity maxima at all of the Leg 78 and Leg 110 sites examined (Tribble, this volume; Pudsey, 1984).

The anomalously high porosity in the lower 15 m of Hole 672A (at the bottom of Site 672) and below 250 mbsf at Site 543 can be attributed to the presence of biogenic silica and to silica cement in the form of opal-CT in lower Eocene sediments. A small amount of cementation strengthens the sediment frame-

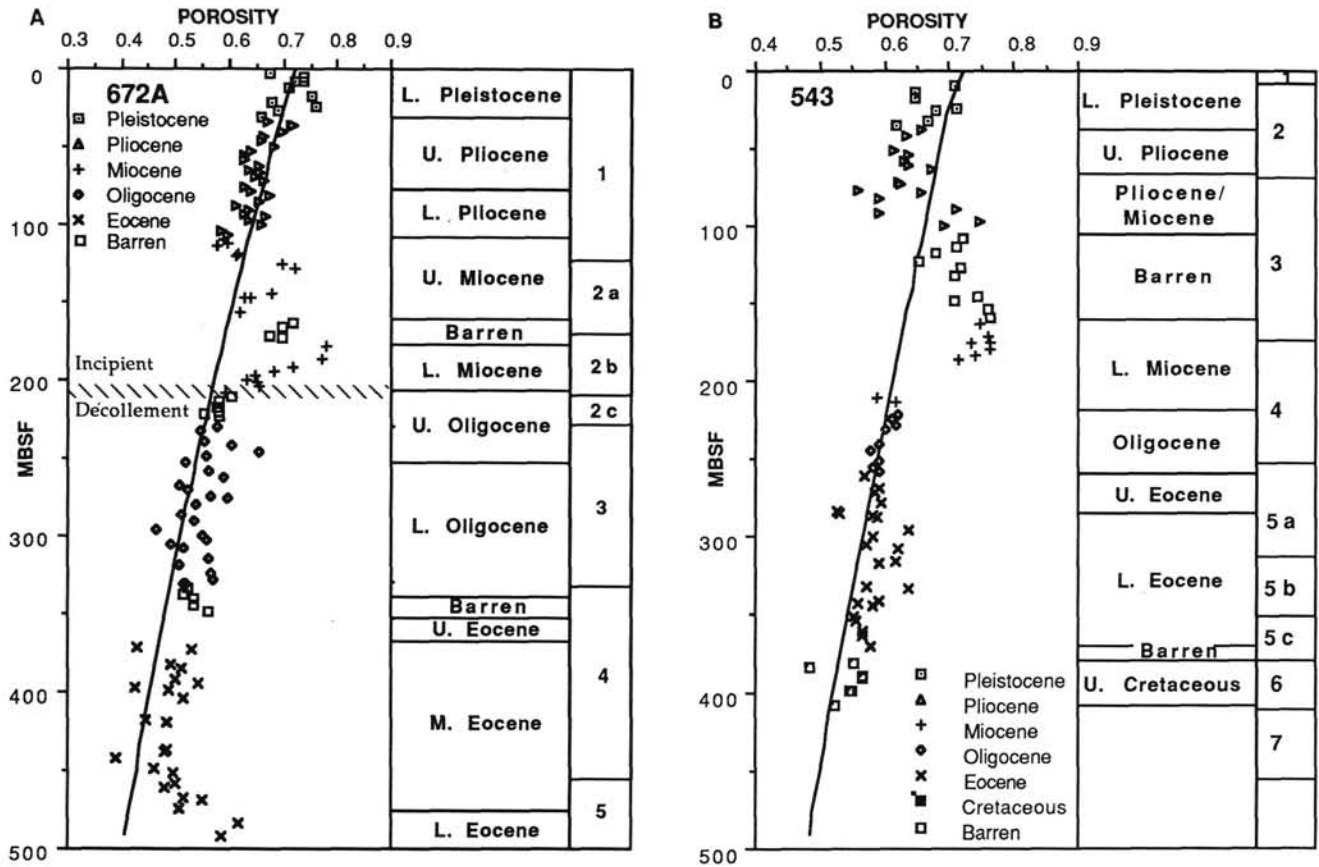


Figure 4. Laboratory porosity vs. depth in Holes 672A (A) and 543 (B). These holes are the reference sections for Legs 110 and 78. The line drawn on the data is Hamilton's (1976) empirical curve for terrigenous silts and clays. The curve was calculated using Hamilton's *in-situ* equations and his estimation of rebound.

work, increasing the ability of the sediments to resist mechanical compaction.

DELTA POROSITY

We now examine the porosity profiles of sites within the accretionary wedge to ascertain how much they diverge from the reference sites. Original data are plotted and tabulated in the individual site chapters (Masle, Moore et al., 1988). To make differences between sites, as well as within sites, more easily comparable, the data are displayed as delta porosity (DP), the difference in porosity between the sample measurements and the porosity predicted by the empirical terrigenous sediment compaction curve (Hamilton, 1976). Negative values of DP indicate porosities less than predicted by the reference curve; positive values, porosities greater than predicted. Hamilton's curve is used in preference to a fit of Site 672 or Site 543 data because of the inhomogeneous nature of the lithologies at the reference sites.

Delta porosity profiles from the two reference sites (672, 543) are plotted in Figure 5. Porosities of smectite-poor non-siliceous sediments at Site 672 generally fall between 0 and 10% less than the values predicted by the terrigenous sediment curve. Pleistocene and Pliocene sediments at Site 543 agree with the Site 672 trend, while the more siliceous Oligocene and older sediments at Site 543 have positive DP values that reflect their different composition.

Located 600 m behind the frontal thrust fault of the wedge (Fig. 1), data from Site 676 (Fig. 6) are similar to the upper part

of the reference sites. The porosity of Pliocene-Pleistocene sediments in the uppermost lithologic unit fall within 0 to -10% porosity. These sediments overlie a local porosity maximum in Miocene age sediments that correlates with the maxima at the reference sites. The *décollement* zone at Site 676 starts at the base of the upper Miocene, Unit 2B, and is composed of a Miocene siliceous mudstone that structurally and lithologically looks much the same as the *décollement* strata penetrated at Site 671. As in the reference sites, increased smectite content corresponds to porosities greater than expected in clay-rich sediments.

Sites 671 and 541 are adjacent to one another, located about 5 km arcward of the tip of accretion-related deformation (Fig. 1). The differential porosity pattern at these two sites is one that is becoming familiar in this discussion (Fig. 7). In the upper parts of the sediment column the porosities of the samples are generally between 0 and 10% less than the reference curve, reflecting no substantial loss of pore volume as compared to the reference sites. Local maxima in porosity occur in Miocene lithologies that are carbonate poor, smectite rich, and are terminated at their lower boundary by a thrust fault. At Site 671 the lower two lithologic units (3 and 4) that lie below the *décollement* contain a relatively greater abundance of coarse-grained continental detritus than sediments being accreted to the prism and appear to have a more significant amount of cementation. Tribble (this volume) suggests that fluid flow from deeper levels of the subduction complex may enhance diagenetic processes in the sub-*décollement* sediments. Increased cementation and/or the presence of opal and smectite may be responsible for the rel-

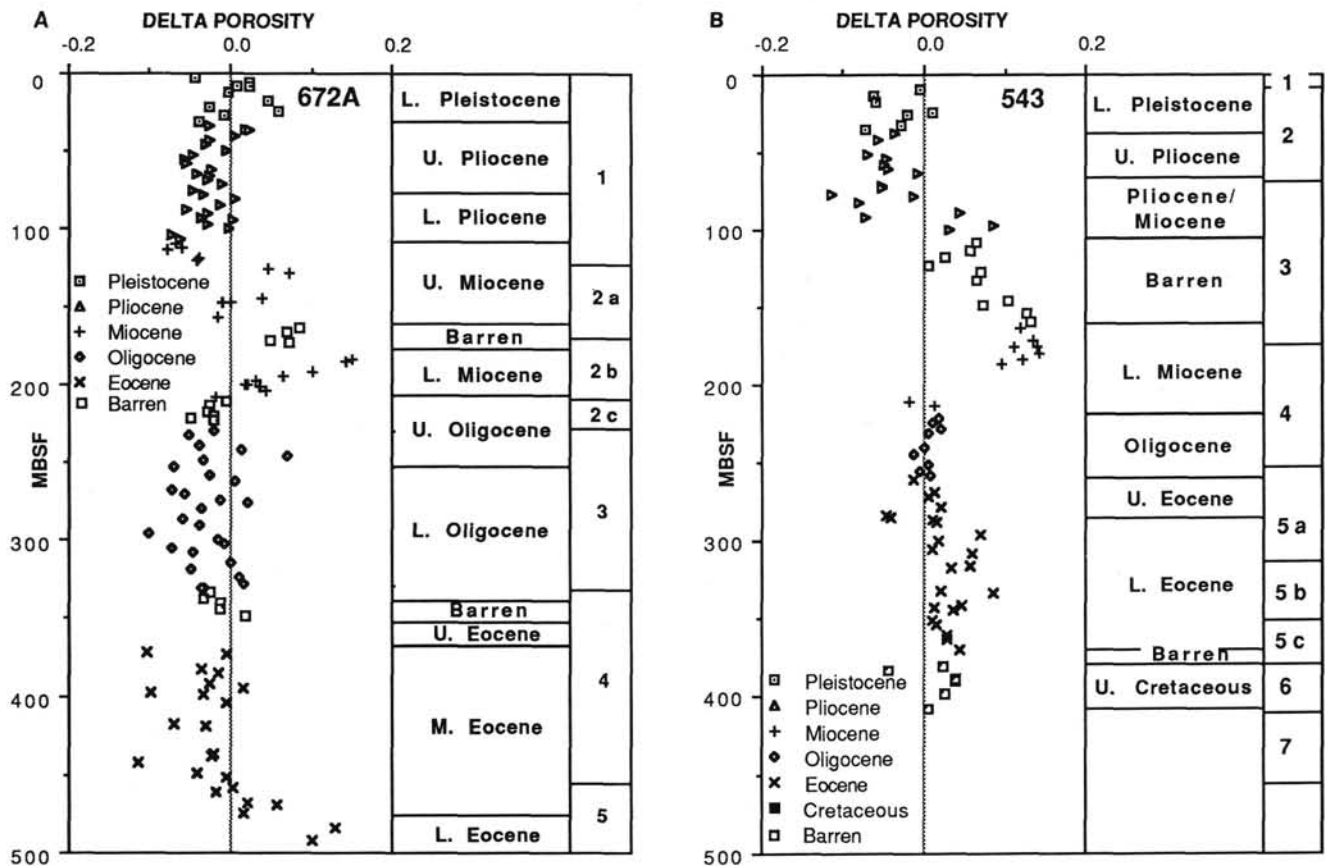


Figure 5. The difference between shipboard measurements of porosity in Holes 672A (A) and 543 (B), and porosity predicted by the terrigenous silt and clay relationship plotted on Figure 4. With the exception of the units discussed in the text, the data generally lie between 0 and -0.10 .

atively high porosity of these units; the cementation strengthens them to resist mechanical compaction in much the same manner as in the lowermost units at Sites 672 and 543.

Farther west and farther into the accretionary complex, Sites 673 and 674 (Fig. 1) offer a look at sediments that have undergone more advanced deformation. Site 673 (Fig. 8) appears to have undergone no water loss as compared to the reference site (672). However, the sediments of Site 673 contain a larger amount of biogenic silica than any of the other sites within the accretionary prism and should perhaps be compared with the more opaline Oligocene and older sediments of Site 543. Site 673 appears to have undergone a reduction of 5% porosity on the basis of comparison to Site 543 data. Site 674 may also reflect a decrease of around 5% porosity through the column. Lithology at this site is closer to that of Site 672, and average differential porosity values are between -5 and -15% . The pattern of relatively high-porosity Miocene sediments overlying faults can also be seen at this site at 90–100 mbsf, and 250 mbsf at Site 674. Closely spaced faults below 250 mbsf make detailed correlation somewhat tenuous for the mostly Oligocene and Eocene sediments at those depths.

Observations of the porosity-depth or differential porosity-depth profiles for sites drilled during Legs 78 and 110 suggest that the amount of dewatering undergone by the sedimentary pile is minimal near the toe of the accretionary wedge. The changes of porosity with depth are generally the same as those seen in other clay-rich sedimentary regimes. Only the two western-most sites (673 and 674) suggest a volume loss, on the order of 5% porosity, when compared to the reference sites.

VELOCITY

Profiles of ultrasonic compressional-wave velocity measurements made on samples at each site are contained in individual site chapters (Masle, Moore, et al., 1988). The compressional-wave velocity of unconsolidated marine sediment is dictated almost entirely by the porosity of those sediments (Wood, 1930). Differences in composition of the sediment are important because of the porosity-depth relationships of differing sediment types (Hamilton, 1976), but intrinsic differences in individual sediment grain elastic moduli have very little effect on the velocity of a mixture dominated by the properties of water. Thus, uncemented sediments of the same porosity will have virtually the same compressional-wave velocity regardless of mineralogy. The compressional-wave velocity of sedimentary rocks, on the other hand, is controlled not only by porosity, but also by the mineralogy of the grains and the extent to which those grains are cemented into a solid framework (Ogushwitz, 1985; Wilkens et al., 1986). It is expected that samples recovered from near the seafloor will behave according to systematics of a seawater-dominated system. Samples from progressively deeper in the sedimentary column will begin to behave more like sedimentary rocks as they lose porosity and become increasingly cemented.

We have chosen two equations to represent end points of the progression from oozes to sedimentary rocks. Wood's equation (Wood, 1930) is used to describe the acoustic velocity of a mixture of loose grains and fluid. The theory assumes that the shear modulus of a high-porosity aggregate of fluid and grains is zero and that its bulk modulus is equal to a geometric average of the

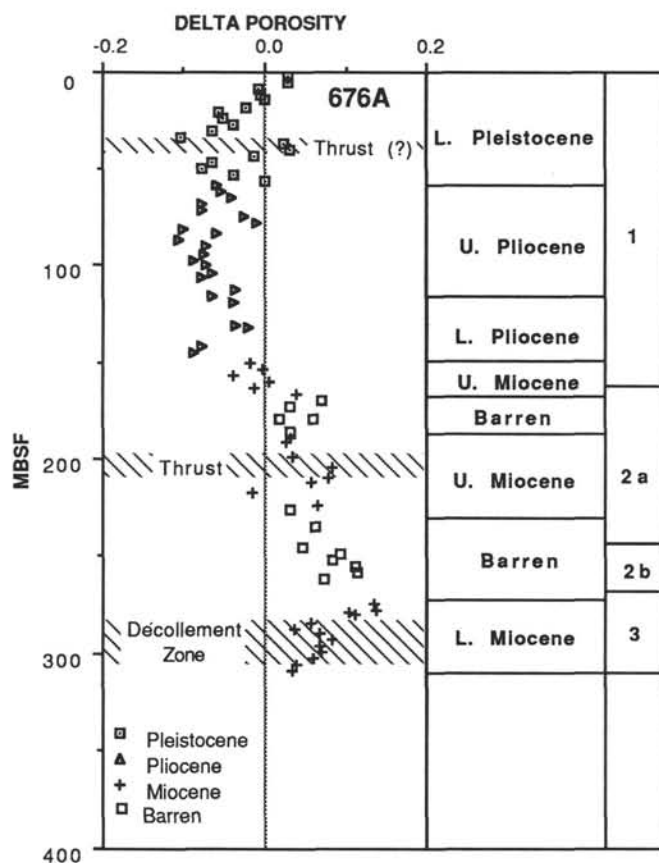


Figure 6. Porosity differential in Hole 676A. Data are relative to an empirical porosity-depth relationship for terrigenous sediments (Hamilton, 1976) plotted in Figure 4.

bulk moduli of the grains and fluid. Wood's equation has been shown to work well in describing the behavior of controlled laboratory clay mixtures of high-porosity material (Ogushwitz, 1985). Hamilton and Bachman (1982) have shown that the zero-shear modulus assumption is probably invalid for marine sediment. The Wood zero-shear modulus assumption for sediments appears less valid as porosity decreases and grain interactions become increasingly strong. However, we use Wood's equation because it represents a limit on porosity-velocity behavior.

The effective bulk modulus of the medium is computed by:

$$K_{sed} = \frac{\Phi}{K_w} + \frac{1-\Phi}{K_g}$$

where K_w is the bulk modulus of seawater, Φ is porosity expressed as a fraction, and K_g is the bulk modulus of the grains. Bulk densities are computed using the densities of seawater and grains. The compressional-wave velocity is computed by:

$$V_p = \sqrt{\frac{K_{sed} + 4\mu/3}{\rho}}$$

where ρ is the bulk density of the seawater-sediment mixture and μ is the mixture shear modulus; assumed here to be zero.

The Wyllie time-average equation (Wyllie et al., 1956) is an empirical formulation based on laboratory data used to represent velocity-porosity relationships for sedimentary rocks. It has

the same form as the Wood equation but uses grain and fluid velocities rather than bulk moduli:

$$V_p = \frac{\Phi}{V_{pw}} + \frac{1-\Phi}{V_{pg}}$$

where the subscripts are as above. The time-average equation has long been used in the petroleum industry for the analysis of acoustic well logs and works reasonably well for sandstones and limestones in the porosity range of about 0 to 30%. The value of velocity obtained from the Wyllie equation for clay-rich sediments of 80% porosity is probably not meaningful in real terms, because the processes that together comprise diagenesis (compaction, dissolution, cementation) all act to substantially reduce porosity such that cemented sedimentary rocks generally have porosities considerably lower than uncemented sediments. As with the porosity-depth function described in the previous section, these curves are used only as standards of reference that adequately describe overall sediment behavior.

The concept of a diagenetically induced change in marine sediment velocity-porosity systematics is illustrated by data from Site 672 (Fig. 9). With the exception of two anomalous samples, velocities of Pliocene, Miocene, and Oligocene samples fall close to the porosity-velocity relationship for uncemented grains. Eocene samples from deeper in the column have velocities that depart from the lower curve and approach the curve depicting sedimentary rock behavior. A new term, "Acoustic Index" or simply "Index", will be used in this study to characterize the extent to which the velocity-porosity behavior of the sediments departs from the behavior of uncemented grains (Wood's equation) and approaches that of sedimentary rock (Wyllie's equation). The Index is defined as:

$$\text{Acoustic Index} = \frac{V_{pmeas} - V_{pWood}}{V_{pWyllie} - V_{pWood}}$$

where V_{pmeas} is the measured velocity, V_{pWood} is the computed velocity of uncemented grains with the same porosity as the sample, and $V_{pWyllie}$ is the computed velocity of a fully cemented shale. Thus a sample whose measured velocity is equal to that predicted by Wood's equation will have an index of 0.0 while a sample with a measured velocity half way between Wood's and Wyllie's predictions will have an index of 0.5.

The difference between the Index and velocity can be seen by examining the Site 672 results (Fig. 10). Between 100 mbsf and the bottom of the Oligocene section (~340 mbsf) velocity exhibits a gradual increase with depth. The porosity in this interval (Fig. 4) generally decreases, with a local maximum in the Miocene centered at about 175 mbsf. The velocity increase with depth is at least partly due to the decrease in porosity, but whether the porosity decrease is totally responsible for the velocity increase is difficult to tell solely from porosity and velocity vs. depth plots. Below 340 mbsf at Site 672, porosity continues to gradually decrease while the velocity gradient increases, suggesting a zone of increased cementation of the grains. Comparing Oligocene and Eocene samples over the same porosity range in Figure 9 shows that most have different velocity-porosity relationships; the deeper, Eocene samples having greater velocities at a given porosity, and thus a larger value of the Index. The Index vs. depth plot shows that Eocene samples behave more like sedimentary rocks than do the younger sediments. Index values suggest that although the mean measured velocity of the Pliocene samples is approximately 1.57 km/s, and the mean velocity for the Oligocene samples is near 1.70 km/s. Most of this velocity increase is due solely to compaction, with the value of the Index remaining virtually unchanged above 340 mbsf.

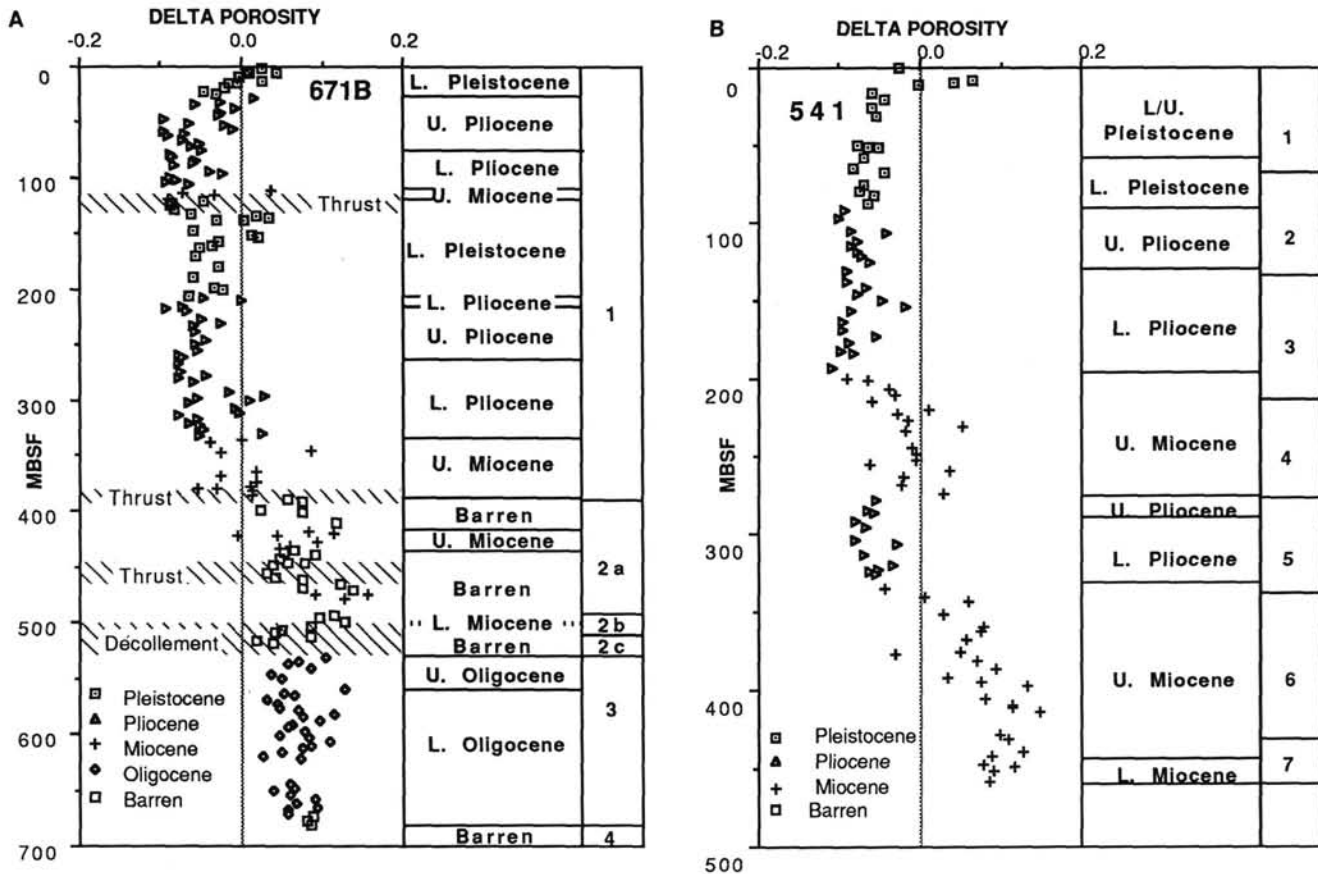


Figure 7. Porosity differential in Holes 671B (A) and 541 (B). Data are relative to an empirical porosity-depth relationship for terrigenous sediments (Hamilton, 1976) plotted in Figure 4. Hole 541 bottomed in the décollement lithology, and Hole 671B penetrated the décollement at approximately 500 mbsf.

Smoothed traces of Index vs. depth for all of the Leg 78 and Leg 110 sites are superimposed in Figure 11. With the exception of the two western-most sites (673 and 674) the trends at all of the sites to depths of about 350 mbsf are remarkably similar. The Index has near-zero values at the tops of the holes; values increase gradually with depth to values around 0.20 at 350 mbsf. The gradual increase is maintained at Site 671 for an additional 200 m and does not change across the décollement zone (500–540 mbsf). This suggests that there is no increase in grain cementation across the décollement at Site 671. Increases in the value of the Index at the bottoms of both Sites 672 and 671 are the result of sampling the cemented lower Eocene sandstones and limestones.

The gradual increase in Index value seen in most of the sites over the upper 350 m may reflect either incipient cementation and/or the inadequacies of the theoretical assumption of a zero-shear modulus in uncemented aggregates. This question cannot be resolved with the data presently available, but it does not alter the conclusion that behavior at all of the sites east of Site 673 is remarkably similar, even though each site has local porosity maxima or compositional variations at different levels in the sediment column.

Sites 673 and 674 exhibit a different Index profile than the other sites. Beneath the slope deposits at the top of each of the sediment columns, the value of the Index increases to around 0.40, indicating a greater degree of cementation at shallow levels than is seen at the other sites. The Index increase is further illustrated in a porosity-velocity plot of Miocene sediments from all of the sites (Fig. 12). Velocity measurements were not made on

Miocene samples from Site 674 because of poor core preservation, but Site 673 data show that, over the same porosity range, Site 673 sediments have higher velocities than Miocene sediments at other sites.

MIOCENE

It is interesting to group Miocene sediments from all sites and to contrast them to sediments of other ages. The Miocene sections are smectite-rich and reasonably uniform in mineralogy (Pudsey, 1984; Tribble, this volume). The Miocene sections generally constitute local porosity maxima wherever they occur. Finally, the Miocene overlies many of the faults (décollement or otherwise) seen at sites east of Site 673.

Porosity and Acoustic Index of Miocene samples are plotted vs. depth in Figure 13. While the sediments at the individual sites exhibited porosity-depth profiles that appeared to parallel the empirical curve shown in Figure 13, it is interesting to note that the Miocene sediments do not have as large a porosity-depth gradient as the reference curve predicts. Profiles of delta porosity of Pliocene, Miocene, and Oligocene sediments are shown in Figure 14. Differences between the Miocene and Pliocene profiles are clear. Pliocene sediments approximate the terrigenous sediment curve (Hamilton, 1976) fairly well with an offset of 0 to 10% porosity. Miocene samples bracket the line $DP = 0$ and tend toward more positive values with increasing depth. Oligocene samples from above the décollement are mostly negative. The different rates of compaction between smectite-rich sediment (Miocene), and smectite-poor sediments (Pliocene, Oligocene) increase the contrast in porosities between Miocene

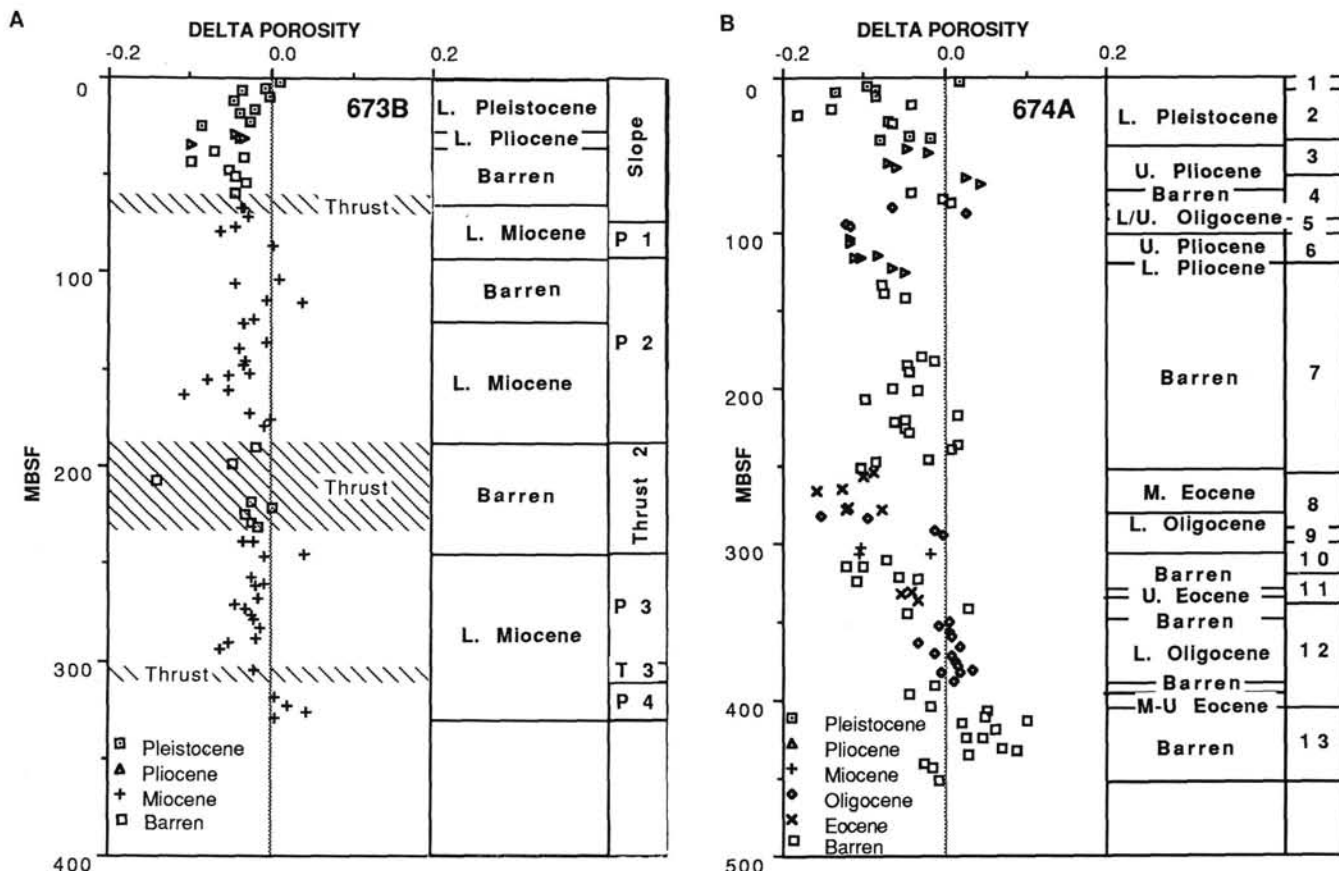


Figure 8. Porosity differential in Holes 673B (A) and 674A (B). Data are relative to an empirical porosity-depth relationship for terrigenous sediments (Hamilton, 1976) plotted in Figure 4.

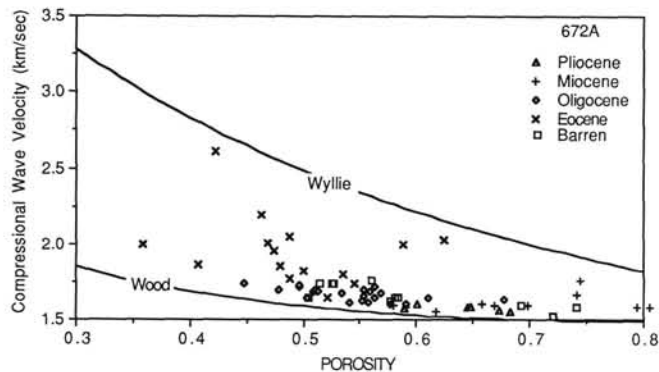


Figure 9. Compressional-wave velocity measured with propagation direction normal to the axis of the core, plotted against sample porosity from Hole 672A. Also included on the plot are two theoretical velocity-porosity relationships: Wyllie's time average equation (Wyllie et al., 1956) and Wood's equation (Wood, 1930). See text for formulas and discussion.

sections and other sections, with depth. We infer that a contrast in sediment porosity means a contrast in sediment strength; the boundaries of Miocene sedimentation will become even greater candidates for faulting as mechanical compaction (burial) progresses.

The Index vs. depth data for Miocene sediments show a gradual increase with depth that parallels the trend seen in all Leg 110 and Leg 78 data east of Site 673 (Fig. 11). A small group of data from Sites 671 and 541 between 420 and 440 mbsf seem to

show a reduction in Index value and relatively high porosity that may be associated with the position of those samples in the vicinity of the décollement and their almost 100% clay content (Masle, Moore, et al., 1988).

CONCLUSIONS

Examination of porosity, velocity, and depth systematics in the light of both empirical and theoretical relationships leads to several conclusions:

1. The initial stages of deformation at the tip of the accretionary prism do not result in a substantial loss of porosity for the accreted sediments. Within 5 km of the toe of the accretionary prism, porosity profiles are similar to profiles at reference sites seaward of the deformation when variations in lithology are considered. Farther from the prism toe, within the accretionary wedge (15–20 km), porosity profiles exhibit a loss of approximately 5% porosity relative to the reference sites.
2. The décollement and most of the other major thrusts penetrated in the prism are associated with Miocene sedimentary sections because of the higher porosity of these sediments and not because of some diagenetic change associated with cementation. The relatively high porosities correlate with abundant smectite derived from volcanic ash alteration.
3. The Miocene lithology appears to compact more slowly than the sediments above and below them. This suggests that the porosity, and probably strength, difference between adjacent units may become greater with depth, resulting in an ever-increasing tendency for the Miocene sediments to be the locus of slip in bedding-parallel faulting events.

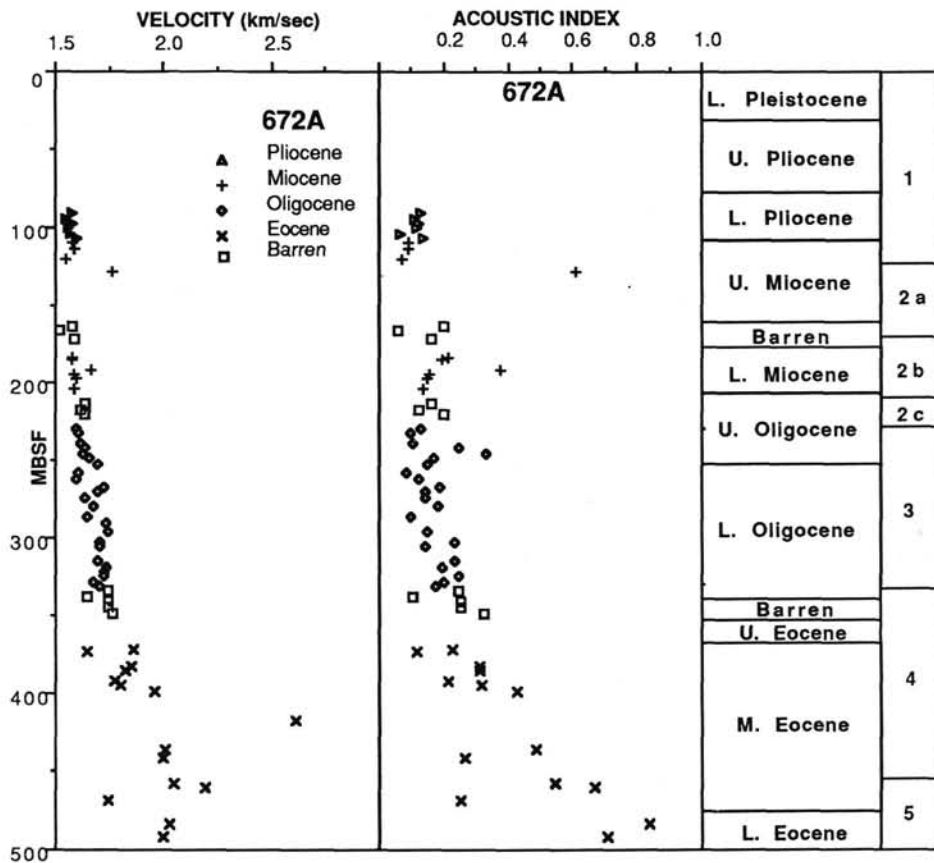


Figure 10. Left: Compressional-wave velocity measured with propagation direction normal to the axis of the core, plotted against depth of sample recovery in Hole 672A. The anomalously fast sample at approximately 130 mbsf is a well-cemented ash layer. Middle: Acoustic Index vs. depth of recovery at Hole 672A. The Index reflects the relative position of a velocity-porosity datum point between theoretical lines shown in Figure 9. Right: Stratigraphy.

ACKNOWLEDGMENTS

This research was partially funded by NSF Grant # OCE-8720032. Thorough reviews by R. von Huene, A. Klaus, and an anonymous reviewer greatly benefitted the manuscript and interpretation of results.

REFERENCES

- Arthur, M. A., Carson, B., and von Huene, R., 1980. Initial tectonic deformation of hemipelagic sediment at the leading edge of the Japan convergent margin. *In Shipboard Scientific Party, Init. Repts. DSDP, 56/57 (Pt. 1):* Washington (U.S. Govt. Printing Office), 569-629.
- Bouma, A. H., and Moore, J. C., 1975. Physical properties in deep-sea sediments from the Philippine Sea and Sea of Japan. *In Karig, D. E., Ingle, J. C., Jr., et al., Init. Repts. DSDP, 31:* Washington (U.S. Govt. Printing Office), 535-568.
- Boyce, R., 1976. Definitions and laboratory techniques of compressional sound velocity parameters and wet-water content, wet-bulk density, and porosity parameters by gravimetric and gamma ray attenuation techniques. *In Schlanger, S. O., Jackson, E. D., et al., Init. Repts. DSDP, 33:* Washington (U.S. Govt. Printing Office), 931-958.
- Bray, C. J., and Karig, D. E., 1986. Physical properties of sediments from the Nankai Trough, Sites 582 and 583. *In Kagami, H., Karig, D. E., Coulbourn, W. C., et al., Init. Repts. DSDP, 87:* Washington (U.S. Govt. Printing Office), 827-842.
- Carson, B., and Bruns, T. R., 1980. Physical properties of sediments from the Japan Trench Margin and outer trench slope: results from Deep Sea Drilling Project Legs 56 and 57. *In Shipboard Scientific Party, Init. Repts. DSDP, 56/57 (Pt. 2):* Washington (U.S. Govt. Printing Office), 1187-1199.
- Carson, B., von Huene, R., and Arthur, M., 1982. Small-scale deformation structures and physical properties related to convergence in Japan Trench slope sediments. *Tectonics, 1:*277-302.
- Davis, D. M., Suppe, J., and Dahlen, F. A., 1983. Mechanics of fold-and-thrust belts and accretionary wedges. *J. Geophys. Res., 88:* 1153-1172.
- Hamilton, E. L., 1976. Variations of density and porosity with depth in deep-sea sediments. *J. Sediment. Petrol., 46:*280-300.
- Hamilton, E. L., and Bachman, R., 1982. Sound velocity and related properties of marine sediments. *J. Acoust. Soc. Am., 72:*1891-1904.
- Hubbert, M. K., and Rubey, W. W., 1959. Role of fluid pressure in mechanics of overthrust faulting. *Geol. Soc. Am. Bull., 70:*115-166.
- Karig, D. E., and Sharnian, G. F., 1975. Subduction and accretion in trenches. *Geol. Soc. Am. Bull., 86:*377-389.
- Lee, H. J., Olsen, H. W., and von Huene, R., 1973. Physical properties of deformed sediments from Site 181. *In Kulm, L. D., von Huene, R., et al., Init. Repts. DSDP, 18:* Washington (U.S. Govt. Printing Office), 897-901.
- Lundberg, N., 1982. Evolution of the slope landward of the Middle America Trench, Nicoya Peninsula, Costa Rica. *In Leggett, J. K. (Ed.), Trench-Forearc Geology:* London (Geol. Soc. London), 131-147.
- Marlow, M. S., Lee, H. J., and Wright, A. W., 1984. Physical properties of sediment from the Lesser Antilles margin along the Barbados Ridge: results from Deep Sea Drilling Project Leg 78A. *In Biju-Duval, B., Moore, J. C., et al., Init. Repts. DSDP, 78A:* Washington (U.S. Govt. Printing Office), 549-558.

- Masle, A., and Moore, J. C., et al., 1988. *Proc. ODP, Init. Repts.*, 110: College Station, TX (Ocean Drilling Program).
- Moore J. C., 1975. Selective subduction. *Geology*, 3:530-532.
- Moore, J. C., and Allwardt, A., 1980. Progressive deformation of a Tertiary trench slope, Kodiak Islands, Alaska. *J. Geophys. Res.*, 85: 4741-4756.
- Moore, J. C., Masle, A., Taylor, E., Alvarez, F., Andreieff, P., Barnes, R., Beck, C., Behrmann, J., Blanc, G., Brown, K., Clark, M., Dolan, J., Fisher, A., Gieskes, J., Hounslow, M., McClellan, P., Moran, K., Ogawa, Y., Sakai, T., Schoonmaker, J., Vrolijk, P. J., Wilkens, R., Williams, C., 1987. Expulsion of fluids from depth along a subduction-zone décollement horizon. *Nature*, 326:785-788.
- Moore, G. F., and Karig, D. E., 1980. Structural geology of Nias Island, Indonesia: implications for subduction zone tectonics. *Am. J. Sci.*, 280:193-223.
- Ogushwitz, P. R., 1985. Applicability of the Biot theory. III. Wave speeds versus depth in marine sediments. *J. Acoust. Soc. Am.*, 77: 453-463.
- Pudsey, C., 1984. X-ray mineralogy of Miocene and older sediments from Deep Sea Drilling Project Leg 78A. In Biju-Duval, B., Moore, J. C., et al., *Init. Repts. DSDP*, 78A: Washington (U.S. Govt. Printing Office), 325-342.
- Schoonmaker, J., Mackenzie, F. T., and Speed, R. C., 1986. Tectonic implications of illite/smectite diagenesis, Barbados accretionary prism. *Clays Clay Miner.*, 34:465-472.
- Shephard, L. E., Bryant, W. R., and Chiou, W. A., 1981. Geotechnical properties of Middle America Trench sediments, Deep Sea Drilling Project Leg 66. In Watkins, J. S., Moore, J. C., et al., *Init. Repts. DSDP*, 66: Washington (U.S. Govt. Printing Office), 475-504.
- Tada, R., and Iijima, A., 1983. Petrology and diagenetic changes of Neogene siliceous rocks in northern Japan. *J. Sediment. Petrol.*, 53: 911-930.
- von Huene, R., and Lee, H., 1982. The possible significance of pore fluid pressures in subduction zones. *AAPG Mem.*, 37:781-791.
- Westbrook, G. K., and Smith, M. J., 1983. Long décollements and mud volcanoes: evidence from the Barbados Ridge Complex for the role of high pore-fluid pressure in the development of an accretionary complex. *Geology*, 11:279-283.
- Wilkens, R. H., Schreiber, B. C., Caruso, L., and Simmons, G., 1986. The effects of diagenesis on the microstructure of Eocene sediments from the area of the Baltimore Canyon Trough. In Poag, C. W., Watts, A. B., et al., *Init. Repts. DSDP*, 95: Washington (U.S. Govt. Printing Office), 527-548.
- Wood, A. B., 1930. *A Textbook of Sound*: London (G. Bell and Sons).
- Wyllie, M.R.J., Gardner, A. R., and Gardner, L. W., 1956. Elastic wave velocities in heterogeneous and porous media. *Geophysics*, 21:41-70.

Date of initial receipt: 29 June 1988

Date of acceptance: 11 April 1989

Ms 110B-116

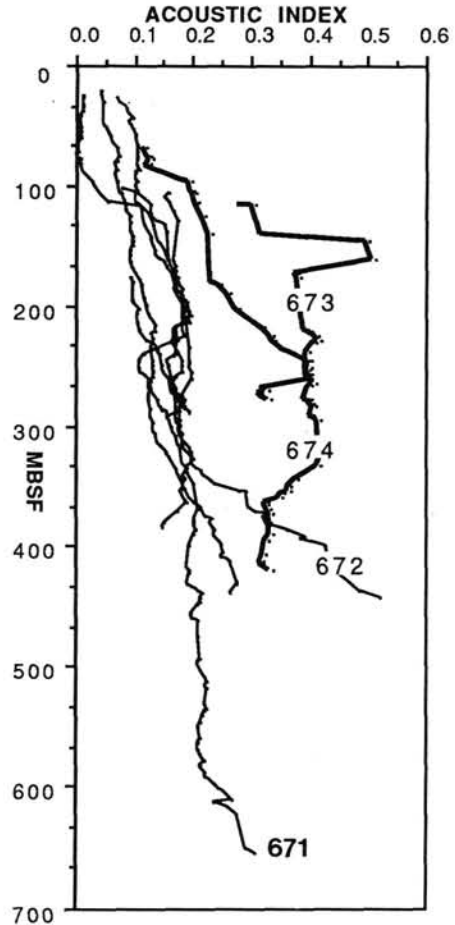


Figure 11. Acoustic Index vs. depth for Leg 78 and Leg 110 sites. Sites 671 and 672 penetrated Oligocene and Eocene sub-décollement lithologies, including cemented sandstones and limestones, resulting in increased Index values at the bottom of each hole. Sites 673 and 674 are clay-rich Miocene sediments much like the lithologies of the upper sections of all the sites.

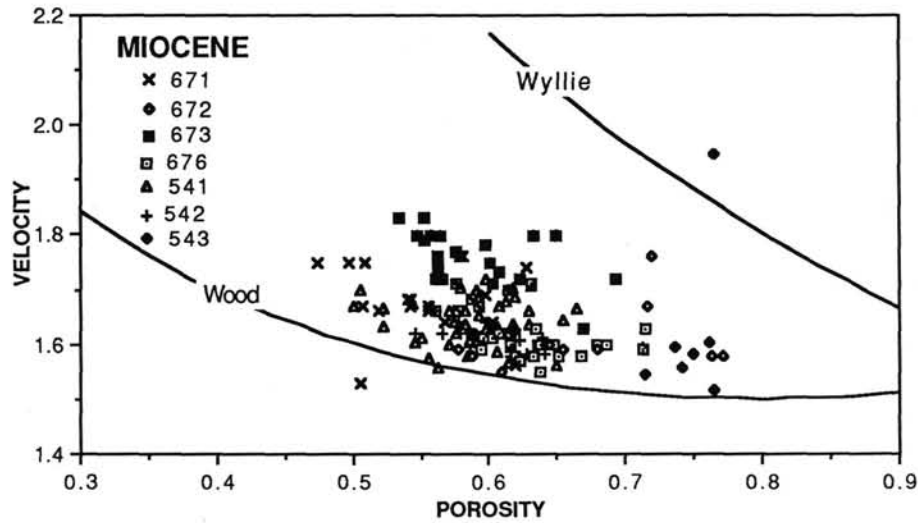


Figure 12. Porosity vs. compressional-wave velocity of Miocene sediments from Leg 78 and 110 sites. Also included on the plot are two theoretical velocity-porosity relationships; Wyllie's time average equation (Wyllie et al., 1956) and Wood's equation (Wood, 1930). See text for formulas and discussion.

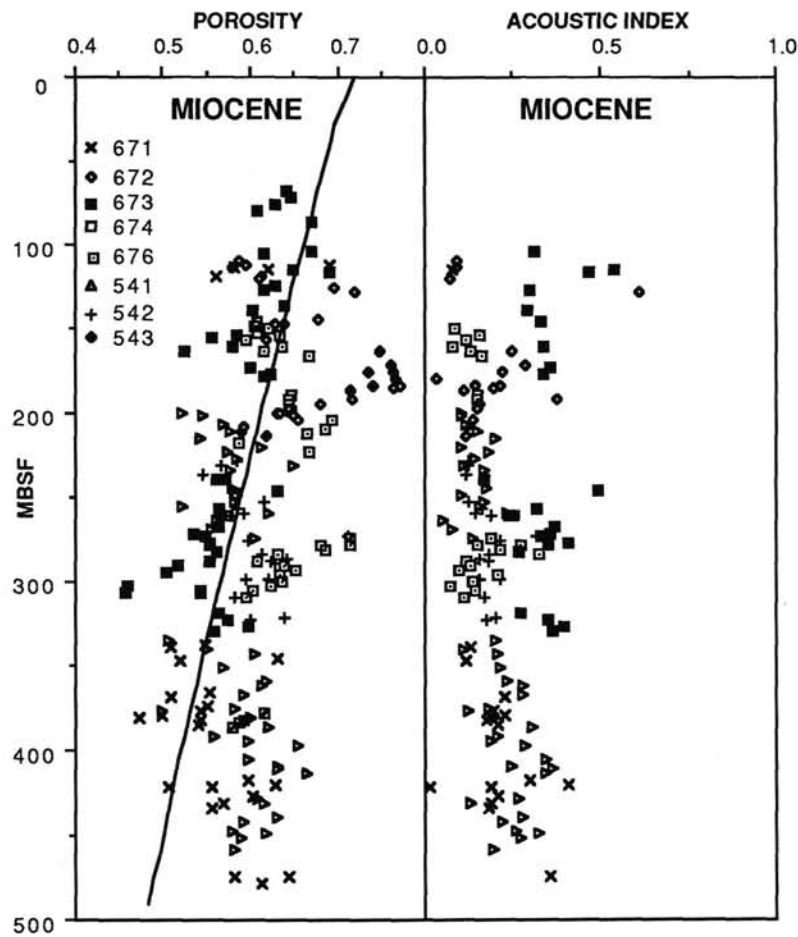


Figure 13. Porosity and Acoustic Index vs. depth for Miocene sediments from Leg 78 and 110 sites. The terrigenous velocity-depth curve is that of Hamilton (1976) and the Index is described in the text.

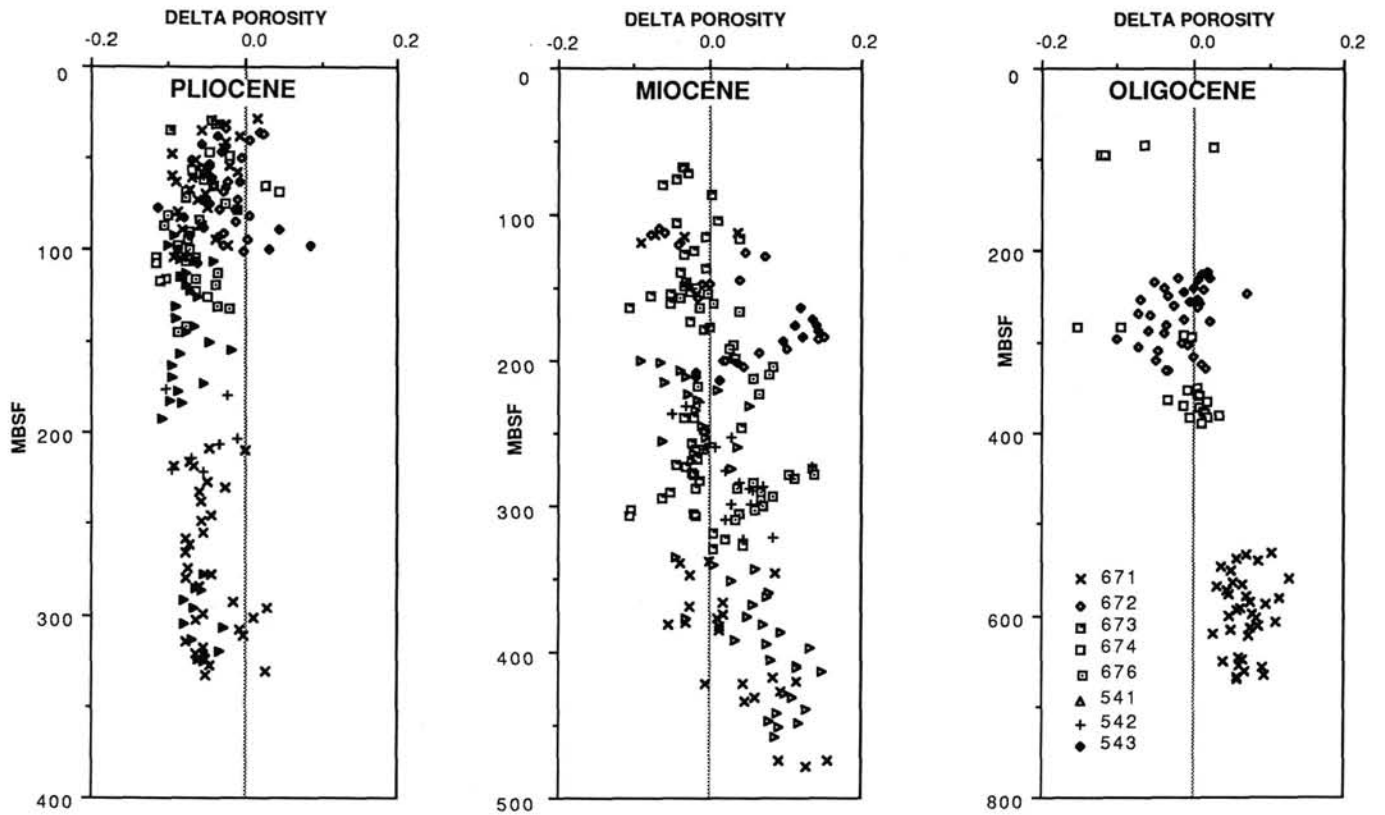


Figure 14. Delta Porosity vs. depth for Pliocene, Miocene, and Oligocene sediments from Leg 78 and 110 sites. Oligocene sediments from Site 671 occur below the décollement and are omitted from this comparison.